The Inference of Atmospheric Ozone Using Satellite Horizon Measurements in the 1042 cm^{-1} Band

JAMES M. RUSSELL III

NASA Langley Research Center, Hampton, Va.

AND S. ROLAND DRAYSON

High Altitude Engineering Laboratory, University of Michigan, Ann Arbor

(Manuscript received 29 April 1971, in revised form 14 September 1971)

ABSTRACT

A method is presented for inferring atmospheric ozone information using infrared horizon radiance measurements in the 1042 cm^{-1} band. An analysis based on this method proves the feasibility of the horizon experiment for determining ozone information and shows that the ozone partial pressure can be determined in the altitude range from 50 down to 25 km. A comprehensive error study is conducted which considers effects of individual errors as well as the effect of all error sources acting simultaneously. The results show that in the absence of a temperature profile bias error, it should be possible to determine the ozone partial pressure to within an rms value of 15–20%. It may be possible to reduce this rms error to 5% by smoothing the solution profile. These results would be seriously degraded by an atmospheric temperature bias error of only 3K; thus, great care should be taken to minimize this source of error in an experiment. It is probable, in view of recent technological developments, that these errors will be much smaller in future flight experiments and the altitude range will widen to include from ~60 km down to the tropopause region.

1. Introduction

Researchers have been trying to develop newer and better techniques for monitoring atmospheric ozone concentrations since Fabry and Buisson's measurements in 1913. A primary reason for the interest in such measurements is the pronounced variation that the vertical ozone profile exhibits as a function of latitude, longitude, day and season. In addition, there is a strong correlation observed between ozone concentration and meteorological conditions (e.g., Dobson, 1930; Paetzold, 1953; Godson, 1960; Duardo, 1967). Furthermore, it is now known that atmospheric ozone is significantly involved, both directly and indirectly, in the fundamental physical processes affecting the energetics and motions of the stratosphere and mesosphere (National Academy of Sciences, 1965).

Most O_3 measurements have been made from the ground, from a balloon, or from a rocket. Some data have also been obtained from satellites, and the satellite is beginning to play a more prominent role in ozone research. All proposed or existing satellite techniques depend on the measurement of energy which has been transmitted, reflected or emitted by the atmosphere in various regions of the electromagnetic spectrum (see, for example, Frith, 1961; Miller, 1969; Dave and Mateer, 1967; Anderson *et al.*, 1969; Hays and Roble, 1967; Prabhakara, 1969; Sekihara and Walshaw, 1969). This paper considers the problem of inferring ozone information from satellite infrared observations. Two types of experiments can be performed: the nadir experiment or the horizon experiment. The nadir approach has been thoroughly analyzed. Prabhakara *et al.* (1970) have used nadir measurements from the Nimbus 3 satellite to infer O_3 data and the general nadir experiment has been studied in detail by Russell (1970). An analysis of the horizon experiment is presented in this study.

The use of infrared measurements of energy emitted along the horizon (or limb) of the earth is an attractive remote sensing approach. It provides the advantage of no background interference since the radiometer measures atmospheric emissions against the blackness of space. This simplifies the analysis as compared to the analysis of nadir measurements because the lower boundary emission term in the equation of radiative transfer (Chandrasekhar, 1960) can be neglected. Furthermore, the horizon experiment affords excellent vertical resolution. Fig. 1 illustrates the geometry. It can be shown that the path length along the line of sight at a given tangent height Z_k is much greater for the tangent layer than for any other layer.[1] Thus, a large percentage of the O_3 mass along the line of sight lies in the tangent layer. In addition to this geometrical

[1] The tangent height is defined as the altitude above the surface where the line of sight makes a perpendicular intersection with the radius vector of the earth.

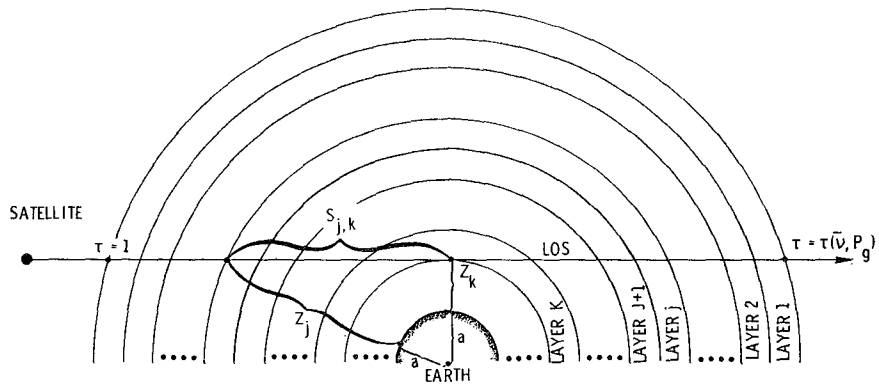

FIG. 1. Horizon geometry (scale distorted).

factor, the ozone density decreases with altitude for levels $\gtrsim 25$ km. These factors acting simultaneously assure that most of the ozone mass, and hence most of the emitted energy, will be concentrated near the tangent point for a large part of the O_3 profile. Consequently, it should be possible to obtain detailed information from horizon measurements regarding the vertical ozone distribution. This is in sharp contrast with the small amount of information which can be inferred from vertically measured radiances (Russell, 1970).

The energy sensed by a limb-viewing radiometer depends on the amount and distribution of the emitting gas as well as the temperature of the atmosphere. Therefore, the temperature distribution must be found before a constituent inversion can be performed. This should be done using simultaneous horizon measurements to obtain temperature data up to a sufficiently high altitude and to obtain time and space correlation between the temperature inferences and other limb measurements.[2] Several authors have analyzed the limb-temperature inversion problem and, as in the nadir experiment, they used the 667 cm^{-1} band of CO_2 (Gille, 1968; McKee *et al.*, 1969a; House and Ohring, 1969; Burn and Uplinger, 1969). Once the temperature profile is known, information regarding the variable gases, H_2O and O_3, can be inferred from measurements in the appropriate absorption bands. House and Ohring (1969) and McKee *et al.* (1969b) used the 315–475 cm^{-1} spectral region to deduce water vapor profiles, and these authors suggested using the 1042 cm^{-1} region to infer ozone information. The purpose of this present work is to evaluate the feasibility of their suggestion.

2. Analysis

a. Basic relations

Calculations in this paper will incorporate the following assumptions:

1) The atmosphere is spherically stratified and spherically symmetric.

2) Scattering at the wavelengths under consideration can be neglected.

3) Atmospheric refraction can be neglected.

4) Ozone is in local thermodynamic equilibrium up to an altitude of 70 km (Kuhn and London, 1969).

All of these assumptions are adequate for the current feasibility study; however, in calculations involving flight data, 1) and 3) will have to be reconsidered. The consequences of assuming spherical symmetry and neglecting refraction have been discussed by Davis (1969) and Bates *et al.* (1967), respectively.

The energy detected by a radiometer aimed toward the horizon is related to the gas concentration and atmospheric temperature through the equation of radiative transfer. If measurements are made at altitudes above the clouds, there is no emission from the lower (or far) boundary since that boundary is space. Therefore, the radiative transfer equation for a single wavenumber $\tilde{\nu}$ and a tangent height Z_k can be written as

$$N_k(\tilde{\nu}) = -\int_1^{\tau(\tilde{\nu},P_g)} B[\tilde{\nu},T(P)]d\tau(\tilde{\nu},P), \qquad (1)$$

where $N_k(\tilde{\nu})$ is the radiance, $B[\tilde{\nu},T(P)]$ the Planck function, and $\tau(\tilde{\nu},P_g)$ the transmittance along the line of sight (LOS) from the satellite to the far boundary of the atmosphere (refer to Fig. 1). The quantity T is atmospheric temperature, P atmospheric pressure, and P_g the pressure at the far boundary. The radiometer field of view in a horizon experiment is very narrow, permitting good vertical resolution. However, atmospheric emissions are weak, resulting in low detected energy, and a wide bandwidth instrument is used to maximize the amount of energy collected. In this case the measured radiance can be represented analytically by the integral of (1) over the range of the radiometer bandwidth, i.e.,

$$N_k = -\int_{\Delta\tilde{\nu}}\int_1^{\tau(\tilde{\nu},P_g)} B[\tilde{\nu},T(P)]d\tau(\tilde{\nu},P)d\tilde{\nu}, \qquad (2)$$

[2] While it may be possible in the future to obtain temperature data up to a high altitude from the nadir experiment, current methods allow accurate temperature inference only up to an altitude of about 30–45 km.

where $\Delta\bar{\nu}$ is the bandwidth. It is assumed in writing (2) that the radiometer instrument function is rectangular over the interval $\Delta\bar{\nu}$. Eq. (2) is the basic relation needed for all remaining calculations in this paper. Since the present work is a feasibility study, transmittances were calculated by the random-experimental band model (Goody, 1952) rather than by the more accurate (but very time consuming) line-by-line method (Drayson, 1966). The absorption line parameters of Clough and Kneizys (1965) were used in these calculations. The average transmittance $\bar{\tau}$ over a spectral interval $\Delta\bar{\nu}$ for a homogeneous path and a Lorentz line shape is given by Goody (1964, Chap. 4) as

$$\overline{\tau_k(\bar{\nu},\bar{P}_{i,k})}=\exp\left\{-\frac{(\beta_{\bar{\nu}}/\bar{d})\bar{u}_{i,k}}{\left(1+2\left[\frac{\beta_{\bar{\nu}}}{2\pi\alpha_{L0}(\bar{\nu})}\right]\bar{l}_{i,k}\right)^{\frac{1}{2}}}\right\}, \quad (3)$$

$i=1,2,3,\cdots$, where $\bar{P}_{i,k}$, $\bar{l}_{i,k}$, and $\bar{u}_{i,k}$ are the effective pressure, length and absorber amount, respectively, and $\alpha_{L0}(\bar{\nu})$ is the Lorentz half-width at the wavenumber $\bar{\nu}$ and at standard temperature and pressure. The quantities $\beta_{\bar{\nu}}$ and $\bar{d}$ are the mean absorption line intensity and line spacing, respectively, for the spectral interval used in the band model calculation. The double i,k subscript in (3) refers to the value in the ith homogeneous layer along the LOS passing through the tangent point Z_k. The homogeneous layer conditions used in (3) were determined in a horizontal direction along the LOS for each tangent point by means of the Curtis-Godson approximation (e.g., Armstrong, 1968.) The Lorentz line shape used in deriving (3) is adequate for the nadir analysis since the optical mass at low pressures is small. But in the horizon experiment, it is possible to have very long paths at low pressures. Therefore, the Voigt profile function (Drayson, 1966) should be included in the calculations. This was accomplished through the use of a correction table published by Gille and Ellingson (1968). The table was developed specifically for correcting transmittances computed with the random-exponential band model and a Lorentz line shape. The corrections were based on values of the quantities

$$Y(\bar{\nu})=\frac{2\alpha_{L0}(\bar{\nu})c}{P_0}\left(\frac{m_{O_3}T_0}{2k\ln 2}\right)^{\frac{1}{2}}\left[\frac{\bar{P}_{i,k}}{(\bar{\nu}\bar{T}_{i,k})}\right], \quad (4)$$

$$R(\bar{\nu})=\left[\frac{\beta_{\bar{\nu}}}{2\pi\alpha_{L0}(\bar{\nu})}\right]\bar{l}_{i,k}Y(\bar{\nu})\pi^{\frac{1}{2}}, \quad (5)$$

where P_0 and T_0 are the pressure and temperature, respectively, at standard conditions, m_{O_3} the mass of the ozone molecule, k Boltzmann's constant, and c the velocity of light. The values of the effective temperatures $\bar{T}_{i,k}$ were computed according to

$$\bar{T}_{i,k}=\frac{\int_0^{\bar{u}_{i,k}}T\,du}{\bar{u}_{i,k}}, \quad i=1,2,3,\cdots. \quad (6)$$

The remaining relationships used in this paper involve the pressure P_k, the geometric length $S_{j,k}$ along the LOS, and the mass path $u_{j,k}$ in a layer of length $S_{j,k}$ (refer to Fig. 1). The pressure is computed according to the hydrostatic relationship

$$P_k=P_0\exp\left[-\frac{M}{R_0}\int_0^{Z_k}\frac{g(Z)}{T(Z)}dZ\right], \quad (7)$$

where M is the mean molecular weight of air and R_0 the universal gas constant. The quantity P_0 is the pressure at the surface of the earth, taken here to be 1013 mb. The quantity $S_{j,k}$ can be computed from the geometry of Fig. 1 and is given by

$$S_{j,k}=[(a+Z_j)^2-(a+Z_k)^2]^{\frac{1}{2}}, \quad j=1,2,3,\cdots, \quad (8)$$

where a is the radius of the earth. The value of $S_{j,k}$ in (8) is the distance from the tangent point out to the boundary of the jth layer. The value of the mass path $u_{j,k}$ corresponding to a horizontal distance $S_{j,k}$ which includes one or more atmospheric layers, can be computed from

$$u_{j,k}=\int_0^{S_{j,k}}\rho(O_3)dS, \quad j=1,2,3,\cdots, \quad (9)$$

or

$$u_{j,k}=\int_0^{S_{j,k}}q\rho\,dS, \quad j=1,2,3,\cdots, \quad (10)$$

where q is the ozone mass mixing ratio, $\rho(O_3)$ the ozone mass density and ρ the atmospheric mass density. Eq. (10) can be further manipulated using the equation of state of an ideal gas to give

$$u_{j,k}=\frac{M}{R_0}\int_0^{S_{j,k}}\frac{qP}{T}dS, \quad j=1,2,3,\cdots. \quad (11)$$

When the mixing ratio is expressed in a form that yields units of atm-cm for $u_{j,k}$, we have

$$q=\frac{A_v}{Mn_s}\frac{P(O_3)}{P}, \quad (12)$$

where A_v is Avogadro's number, n_s the number density of air at standard conditions, and $P(O_3)$ the ozone partial pressure. Inserting (12) into (11) gives

$$u_{j,k}=\frac{A_v}{R_0n_s}\int_0^{S_{j,k}}\frac{P(O_3)}{T}dS, \quad j=1,2,3,\cdots. \quad (13)$$

The absorber amounts computed by (13) are for one-half of the atmosphere on either side of the tangent point along the LOS. The values for the opposite half of the atmosphere are the mirror images of the values for the first half since spherical symmetry is assumed.

b. The inversion method

The purpose of this section is to develop a method for inferring an ozone profile starting with a measured horizon radiance profile and a known temperature distribution. It would appear that it is possible to infer the entire O_3 profile since as the radiometer scans the limb from the top of the atmosphere downward, it views a different layer of the horizon at each new tangent point. However, it may be difficult to recover all of the O_3 profile in this way. At each successively lower tangent point, the radiometer must look through the atmosphere above that point, and the atmosphere from above could mask any new information provided by energy coming from the lower layer. For example, if the atmosphere becomes opaque at some low altitude, it would be impossible to infer information about the new layer. Thus, it can be expected that there will be a lower limit to the limb technique regardless of the limit which arises because of clouds. This will be discussed in more detail later.

The so-called "onion peeling" approach will be used in this study to develop the inversion procedure. The atmosphere is divided up into layers and the inversion begins with the highest layer for which there is a measurable radiometer signal. Once the inversion is complete in the first layer, the next lowest layer is added and an inversion is performed for that layer. This procedure continues until the lower altitude limit is reached. This is the approach followed by McKee *et al.* (1969a, b). The initial step in the solution procedure for the current work is to make a linear approximation for the relationship between the measured radiance, the calculated radiance, and the ozone partial pressure at the lower boundary of a layer as follows:

$$N_{mk}=N_{ck}+\frac{\partial N_{ck}}{\partial P(O_3)}\Delta P(O_3), \tag{14}$$

where, as before, the k subscript refers to the kth tangent point. Eq. (14) is a truncated Taylor series expansion. The quantities N_{mk} and N_{ck} are the measured and calculated radiances, respectively, $P(O_3)$ the ozone partial pressure at the bottom of a layer, and $\Delta P(O_3)$ a perturbation parameter. The final value of the O_3 partial pressure is determined by iteration. The procedure begins with a guess for $P(O_3)$ at the bottom of the first layer. Next, the partial pressure is computed at the bottom of each successive higher layer assuming a constant O_3 mixing ratio. After this, N_{ck} is calculated using (2), the partial derivative is determined by letting $P(O_3)$ change by a small amount, and (14) is solved for the perturbation term $\Delta P(O_3)$ according to

$$\Delta P(O_3)=\Delta N\left[\frac{\partial N_{ck}}{\partial P(O_3)}\right]^{-1}, \tag{15}$$

where ΔN is the difference $(N_{mk}-N_{ck})$. The quantity $\Delta P(O_3)$ is then added to the original guess for $P(O_3)$ and the process continues until some convergence criteria (to be specified later) are met. Once $P(O_3)$ is known for the first layer, it is used as an initial guess for the partial pressure at the bottom of the next lowest layer and the iteration is performed for that layer and so on. In reality, the quantity ΔN contains errors; measurement errors arise in N_{mk}, and all other errors occur in determining N_{ck}. Therefore (15) can be expressed in the form

$$\Delta P(O_3)=\frac{\Delta N}{D}+\frac{\epsilon}{D}, \tag{16}$$

where ϵ represents the equivalent radiance error and D is the derivative $\partial N_{ck}/\partial P(O_3)$. The reason for a lower altitude limit is now clear. As the radiometer probes deeper and deeper into the atmosphere, the derivative D continually decreases because the ozone absorption across the horizon approaches opacity. Consequently, the error term is magnified. In the extreme, if opacity is reached, a solution is not possible since D will equal zero. Eq. (16) is a mathematical statement of the discussion in the first part of this subsection regarding a lower altitude limit to the horizon technique. This can also be illustrated using the vertical weighting function along a LOS. This function is defined by the change in transmittance along the LOS with respect to the vertical coordinate Z and it shows the approximate distribution of energy being emitted along the LOS. If the function is greatest at the tangent point, then the energy emitted along the LOS is localized near the tangent point and the inversion will not be very sensitive to errors. If, on on the other hand, the function peaks somewhere else and is broad, then the energy emitted by the atmosphere is distributed all along the LOS and an inversion will be difficult. Since every altitude except the tangent point altitude is crossed twice during a horizontal pass through the atmosphere, the weighting functions anterior and posterior to the tangent point must be summed in computing the total vertical weight. Thus, we have

$$W_k(Z)=\left|\overline{\frac{\partial\tau(\Delta\bar{\nu},Z)}{\partial Z}}\right|_a+\left|\overline{\frac{\partial\tau(\Delta\bar{\nu},Z)}{\partial Z}}\right|_p, \tag{17}$$

where $W_k(Z)$ is the weighting function for a LOS passing through Z_k, subscripts a and p denote anterior and posterior, respectively, and the vertical bars denote absolute values. The $\Delta\bar{\nu}$ argument indicates that the transmittance is averaged over the instrument band

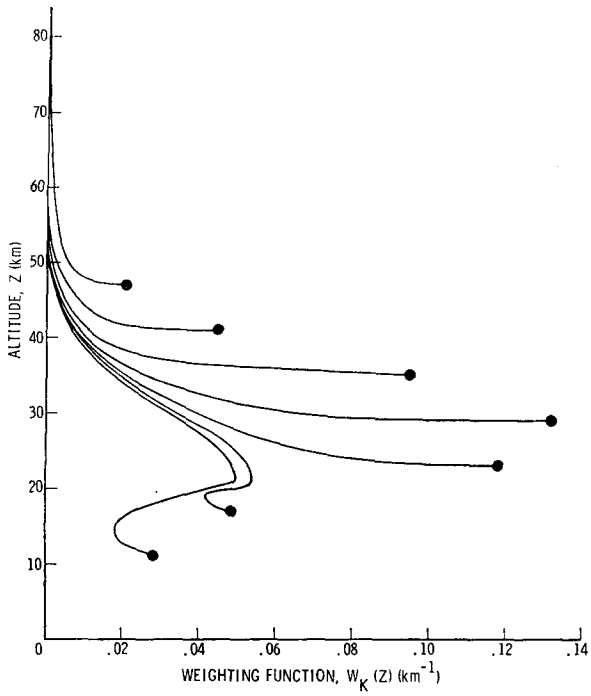

FIG. 2. Vertical weighting function $W_k(Z)$ over the interval 995 to 1070 cm^{-1} for a high-latitude O_3 profile. Dots indicate tangent heights.

pass of width $\Delta\bar{\nu}$; values of 5, 15, 25 and 75 cm^{-1} were used in this study. Eq. (17) with $\Delta\bar{\nu}=75$ cm^{-1} is plotted for various tangent points and a high-latitude ozone profile in Fig. 2. The figure shows that it will be difficult to infer O_3 information at altitudes $\lesssim 25$ km. For example, the radiance measured on a LOS passing through $Z_k=17$ km would not arise mainly from near the tangent point but would, instead, come from points all along the LOS covering the vertical range 17 to 50 km. The weighting functions can be improved by confining calculations to one of the weakly absorbing band-wing regions such as from 995 to 1020 cm^{-1}. However, this is also accompanied by a loss of signal which tends to offset any gain. This is discussed in the next section. Plots of $W_k(Z)$ for a low latitude O_3 profile are similar to those shown in Fig. 2. Thus, scanning from the top of the atmosphere downward, the inversions should become increasingly sensitive to errors for successively lower tangent points since the proportion of the measured radiance which arises in the tangent layer will continually diminish. The prospects do not appear to be very good for obtaining ozone information in the lower stratosphere. These results suggest that an inversion will be feasible in the lower region only when the radiance noise is very low and other errors are small. The sensitivity of the inversion technique to various errors is studied in the next section for the entire range of the ozone profile down to the tropopause.

TABLE 1. Types and ranges of errors used for the analysis of individual error effects in the horizon experiment.

Type of error	Range
Random radiance noise, normally distributed with a mean of zero	$\sigma=0.02$ W $(m^2\text{-sr})^{-1}$
Radiance bias	± 0.03 W $(m^2\text{-sr})^{-1}$
Radiance scale	$\pm 3\%$
Tangent height	± 1 km
Ozone absorption line intensity	$\pm 15\%$
Surface pressure	$\pm 5\%$
Temperature bias	± 3K

3. Error study

The first step in the error analysis was the computation of synthetic horizon radiance profiles. This was done using Eq. (2) and ozone and temperature profiles measured by the Air Force Cambridge Research Laboratories (Hering and Borden, 1967). These

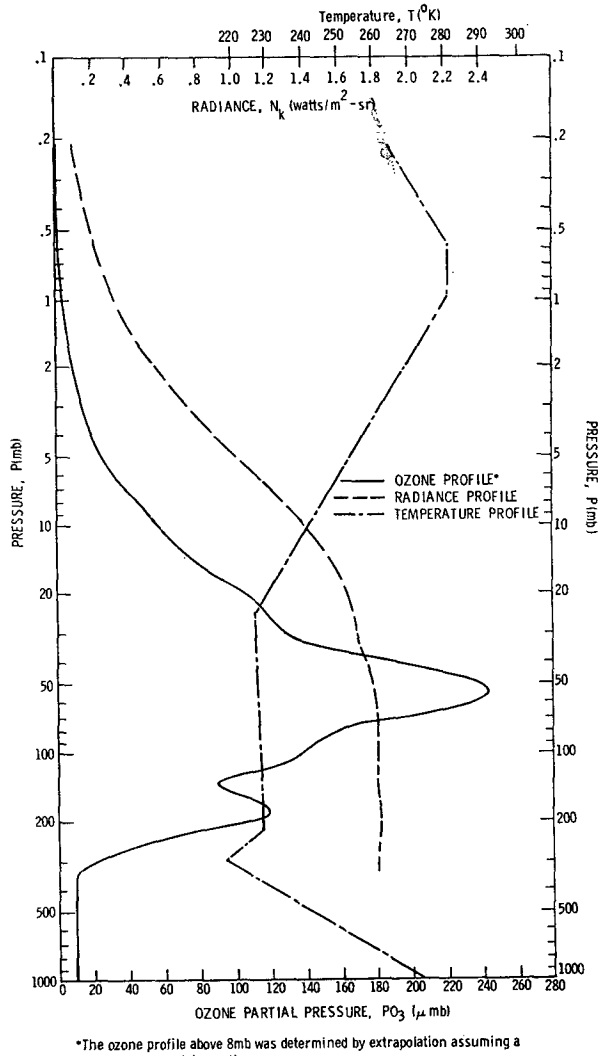

FIG. 3. Ozone, radiance and temperature profiles for a Thule, Greenland (76.5N), sounding, 19 May 1965.

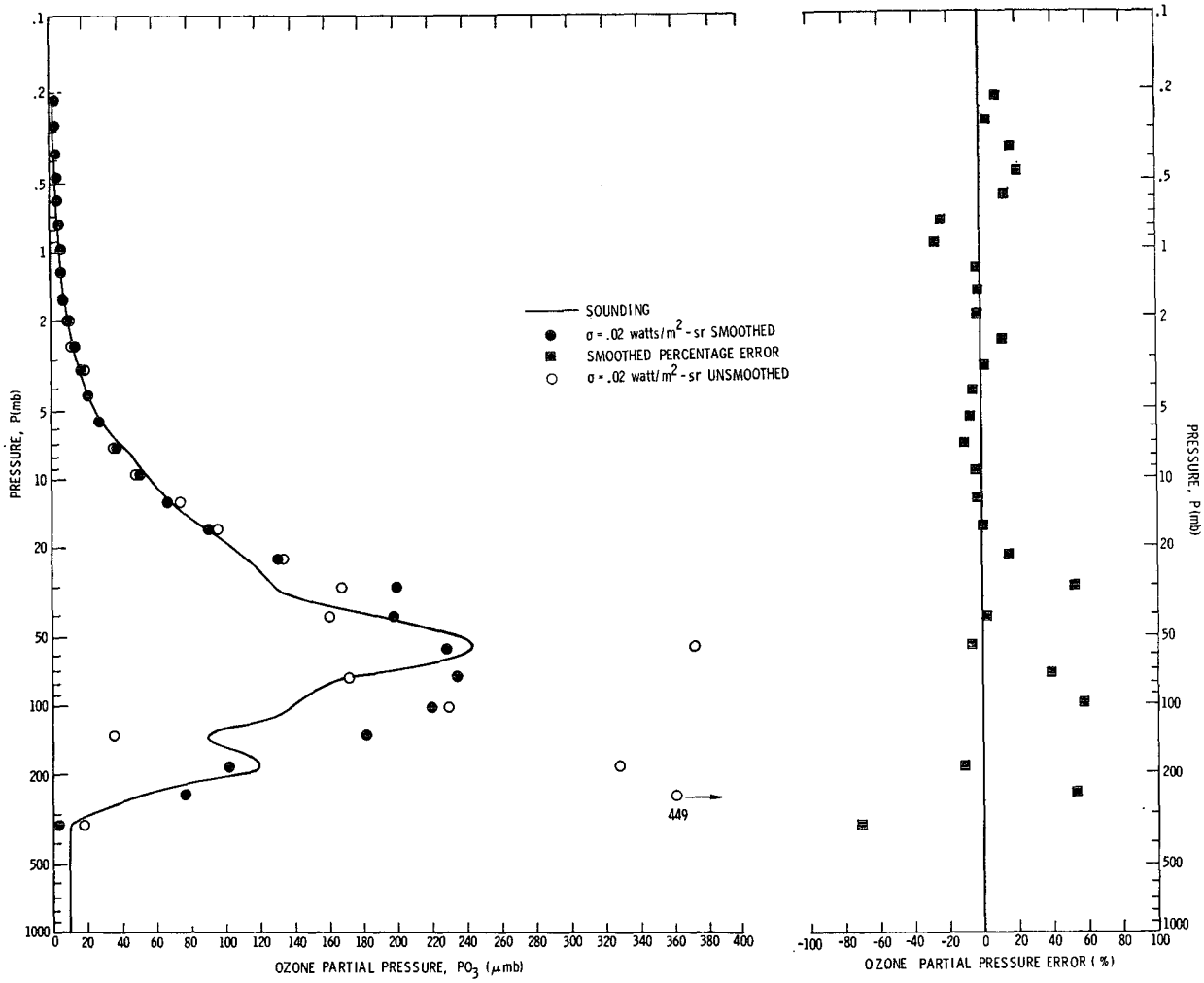

FIG. 4. Radiance random noise results for Thule, Greenland (76.5N), 19 May 1965.

synthetic profiles were then taken as "measured" values in studying the inversion technique. Transmittances used in the calculations were determined for a temperature[3] of 250K. Spectral radiances were computed at 5 cm^{-1} intervals throughout the absorption band and these values were integrated against wavenumber to give the total radiance. The calculations were performed for 2-km thick layers. This thickness gave radiance differences for two successive tangent points which were sufficiently above the anticipated noise level of a practical radiometer and provided, at the same time, sufficient vertical resolution to define the ozone profile. Convergence criteria were imposed on the difference, $\Delta N = N_{mk} - N_{ck}$, and on the perturbation parameter $\Delta P(O_3)$. The iteration was stopped when either $\Delta N \leqslant 0.01$ W $(m^2\text{-sr})^{-1}$ or $\Delta P(O_3) \leqslant 0.1\,\mu$mb. These limits were selected to give sufficient accuracy in a minimum of computing time.

[3] Calculations showed that the variation of transmittance with temperature has a negligible effect on the total band radiance for a given tangent point.

The error study was designed to establish the lower altitude limit of the inversion approach and to identify those errors which have the greatest effect on the results. Errors in various quantities were added one at a time and inversions were performed to determine the effects. The types and ranges of errors used are given in Table 1. The types of error are those which normally would be encountered in an actual experiment and the ranges include values which allow clear identification of the most important error effects. The first series of calculations were performed for a Thule, Greenland (76.5N), sounding. The ozone, temperature and horizon radiance profiles used in the computations are shown in Fig. 3. These data represent typical high-latitude conditions. A series of calculations were also made for a low-latitude sounding and these results are discussed later. The effects of specific errors are considered in the following paragraphs.

The inversion of the radiance profile of Fig. 3, using perfect radiance values, reproduced the O_3 profile to within approximately 0.2 μmb at every inversion point.

The result with random noise added to the radiances is shown in Fig. 4 by clear circles. The figure shows that the solution becomes intolerably sensitive to noise near the level of the primary maximum in the profile. A reduction of these errors was accomplished by using segmented quadratic smoothing of the radiance data. The radiance profile was separated into three segments and a quadratic was fitted, in a least-squares sense, to each of the segments. The end point of the first quadratic solution was used as the beginning point in finding the next, and an average value was taken at the end point of the overlapping quadratics to reduce the magnitude of any discontinuity present. The solid circles are the inversion results using data smoothed in this manner. The results are still strongly affected by the noise but they represent a substantial improvement over the solution obtained using unsmoothed data. Percentage errors in ozone partial pressure are also plotted in Fig. 4 and all following figures where appropriate. Similar results using radiances for Green Bay, Wisc., and Albrook Field, Canal Zone, soundings are shown in Figs. 5 and 6, respectively. The inversions in an actual experiment may not be as poor as these results indicate since practical noise levels will probably be only one-half the value used in the calculations (McKee *et al.*, 1969b).

The Thule, Greenland, calculations were repeated using the ranges 995–1000 cm^{-1}, 995–1010 cm^{-1}, and 995–1020 cm^{-1}. This was done to determine if the sensitivity of the inversion to noise could be reduced by using a wing of the band rather than the entire width. A fair improvement in the weighting functions resulted; however, the signal level was reduced and there was no improvement in the solution for the same noise level as used previously. These calculations indicate that in order to sound below the maximum of the ozone profile, the noise level will have to be lower than that used in this study.

The error in O_3 partial pressure for a tangent height error is shown in Fig. 7. In this calculation, a +1 km

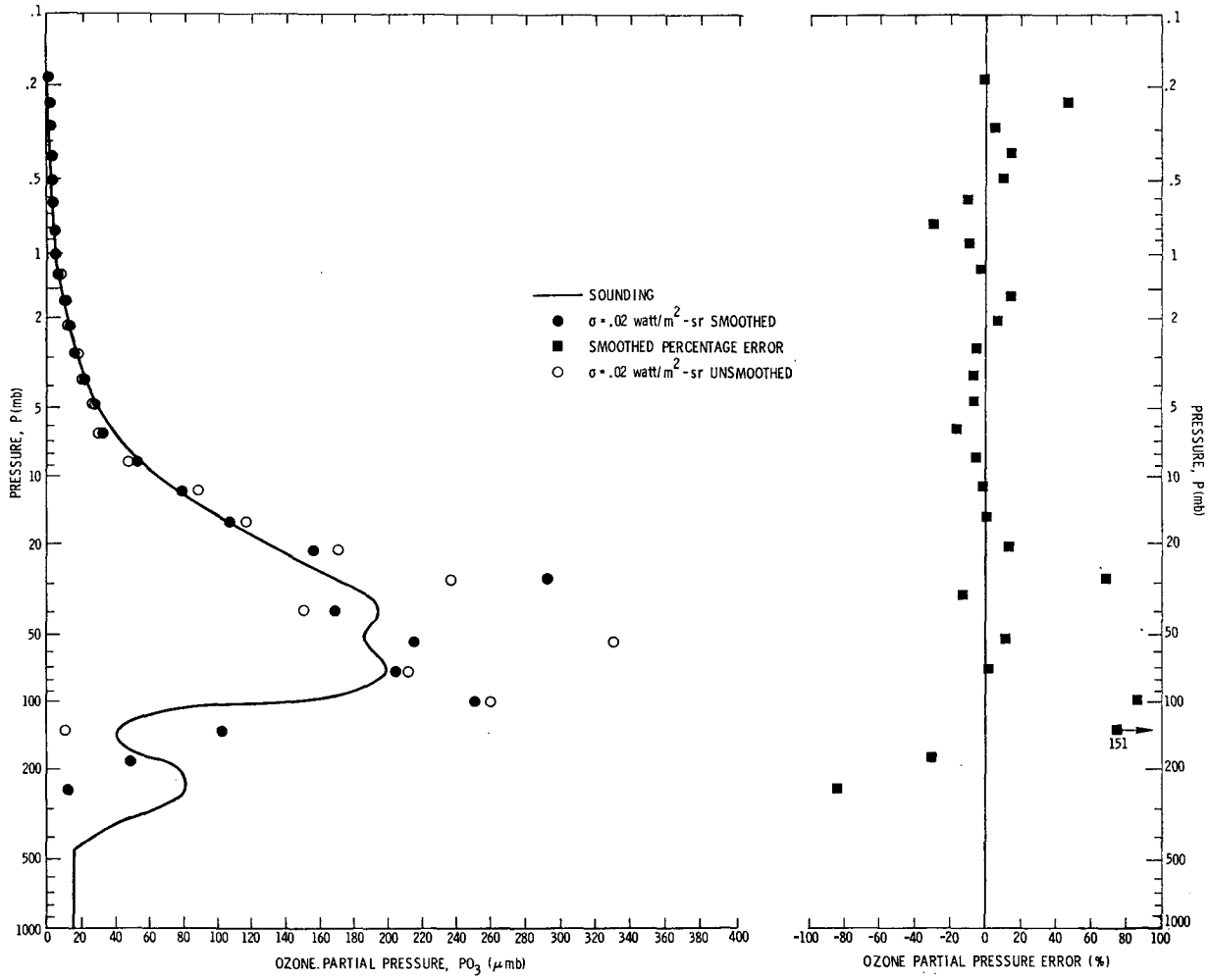

FIG. 5. Radiance random noise results for Green Bay, Wisc. (44.5N), 15 March 1965.

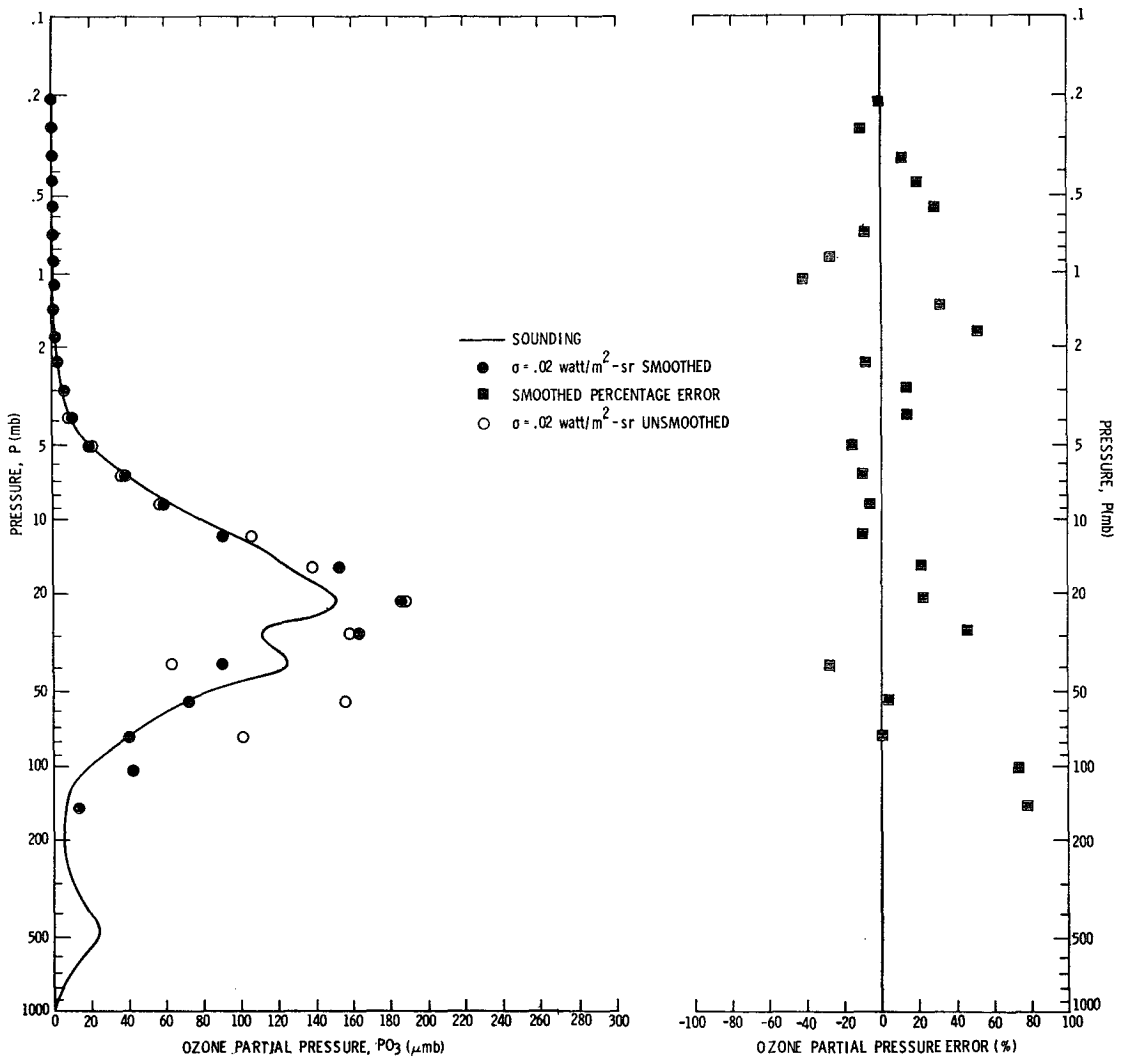

FIG. 6. Radiance random noise results for Albrook Field, Canal Zone (9N), 28 July 1965.

tangent height error means that each radiance value is measured at a tangent point 1 km higher than the altitude used in the inversion calculations; for a -1 km tangent height error the converse is true. Thus, with a $+1$ km error the entire curve is shifted downward and with a -1 km error it is shifted upward. Again, the resulting error in O_3 partial pressure is magnified significantly at higher pressures. At 30 mb, the errors in $P(O_3)$ are $+23\%$ and -11%; at 40 mb they are $+7\%$ and -10%; and at 60 mb they are $\pm 42\%$ and increase at higher pressures. A ± 1 km tangent height discrepancy is realistic for current experiments (McKee *et al.*, 1969b).

The resulting inversions for temperature bias errors of ± 3K are shown in Fig. 8. This error source causes a larger ozone error than any other single factor for the error magnitudes considered in this report. This is because the radiance emitted by the atmosphere is such a strong function of the temperature. The ozone errors at 30 mb are -40% and $+110\%$. As the pressure is increased further the error rapidly increases, and for a negative temperature bias it becomes infinite. The instability arises because a negative temperature bias requires an increased O_3 partial pressure to give the same atmospheric emission as when the temperature error is zero, and, in this case, the required increase is so great that the atmosphere becomes opaque. The sensitivity of the inversion to this error source is critical.

The effects of $\pm 15\%$ errors in ozone absorption line strength are shown in Fig. 9. The errors in O_3 partial pressure at 30 mb are $\pm 15\%$ and they change only slightly for higher pressures. Percentage error is not plotted in Fig. 9 since the value is approximately constant throughout the altitude range under consideration. Currently, absorption line strength errors may be as high as 35% in parts of the band, but our calculations show that the errors in approximately one-half of the band are about equal and opposite to errors in the other

half. Thus, the effects of these errors tend to cancel when the total band radiance is computed. Regardless of this effect, the O_3 partial pressure error caused by an error in line strength should eventually be decreased to 4% or less after the physics of the ozone molecule becomes more completely understood.

The errors in O_3 partial pressure for radiance bias errors of ± 0.03 W $(m^2\text{-sr})^{-1}$ and surface pressure errors of $\pm 5\%$, are similar in magnitude and effect to the errors shown in Fig. 9. The effects of $\pm 3\%$ radiance scale errors are shown in Fig. 10. According to McKee *et al.* (1969a), it is currently possible to control practical radiance errors to within one-third of these values. Also, data presented by Smith *et al.* (1963) indicate that the surface pressure in the Northern Hemisphere is known from climatology most of the time to within about 2% or less. Thus, ozone errors which come from these sources probably will be small. Using practical error levels as estimates, it is predicted that the maximum ozone error caused by any one of these errors will not exceed 7% at 25 mb and it will be smaller at lower pressures.

Fig. 10 concludes the analysis of individual error effects using high-latitude data. The error calculations were repeated for radiances computed from a Canal Zone sounding to determine if any latitudinal effects exist regarding the error sensitivity of the inversion. There was virtually no difference in results for the upper stratospheric region; but in the middle stratosphere, the ozone error was smaller than the corresponding high-latitude results in every calculation. As an example, the ozone errors at 25 mb for a ± 3K temperature bias error are -37% and $+70\%$ for low-latitude calculations as compared with -40% and $+100\%$ for the high-latitude results. The ozone error for a negative temperature bias never reached 100% at any point which contrasts sharply with the infinite error obtained for the Thule, Greenland, inversion. The reduced error magnification is due to a combination of effects which arise because of the shape of the temperature profile

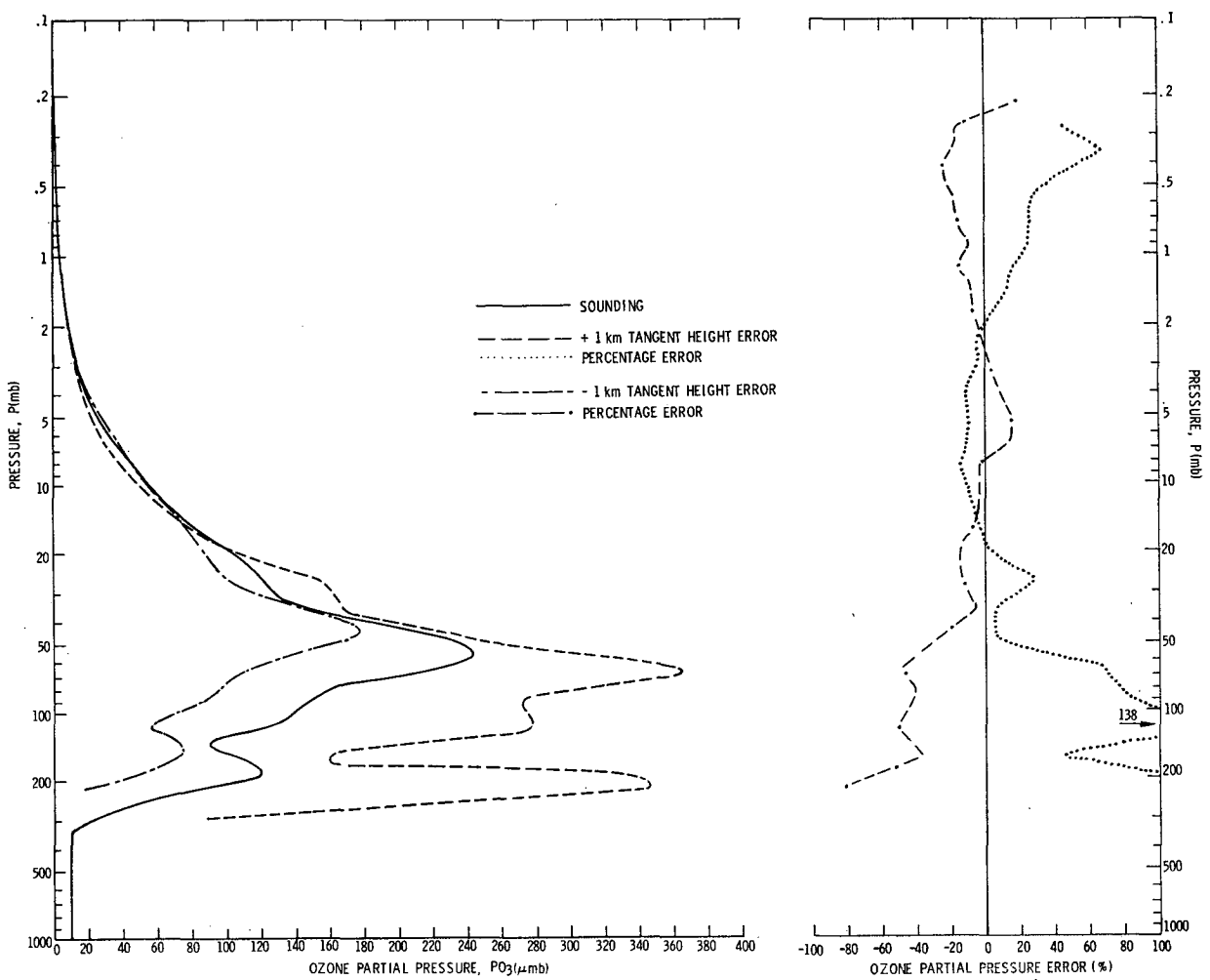

FIG. 7. Tangent height error results for Thule, Greenland (76.5N), 19 May 1965.

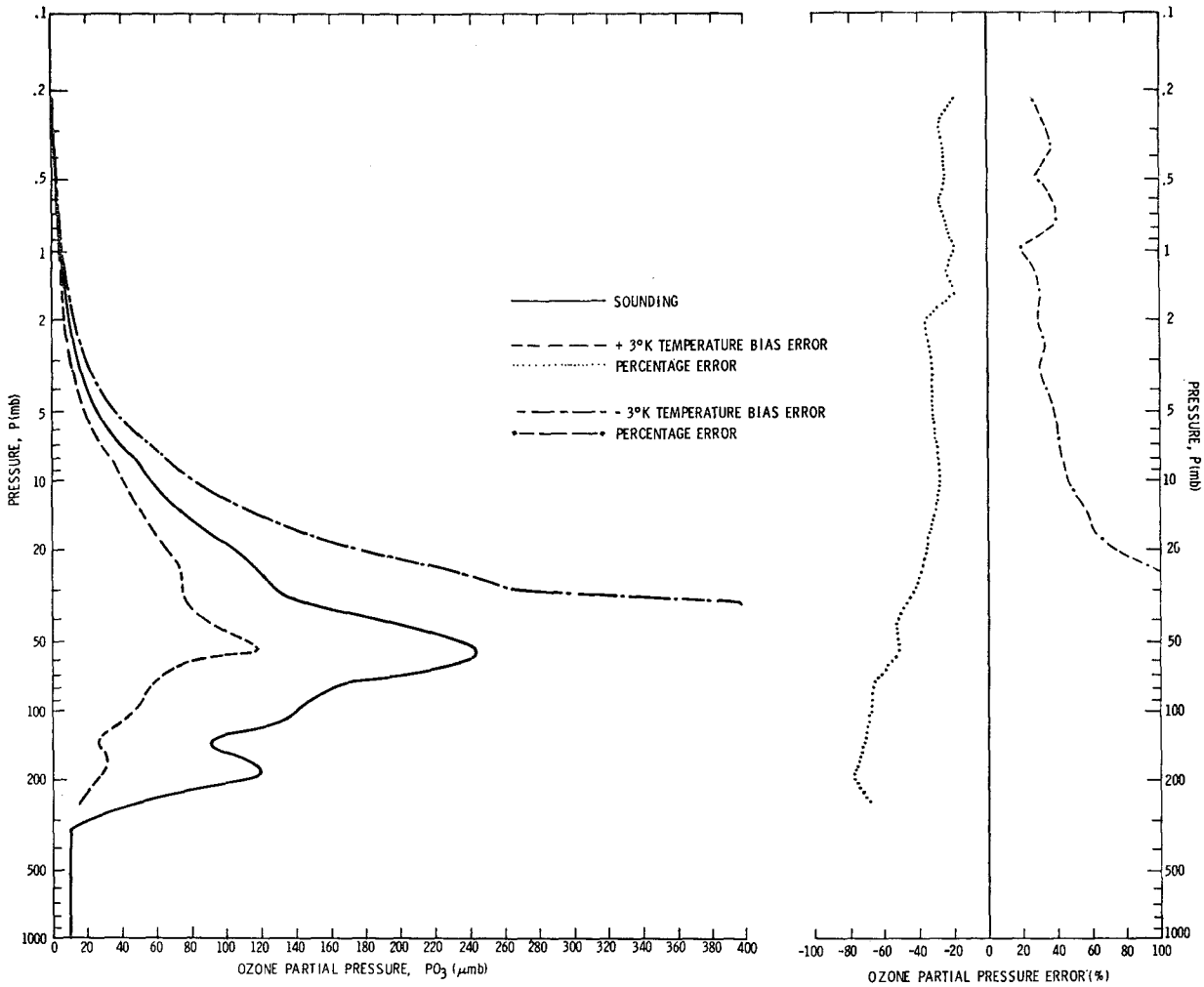

FIG. 8. Temperature bias error results for Thule, Greenland (76.5N), 19 May 1965.

and the greater transparency of the atmosphere at low latitudes. The greater transparency occurs since, characteristically, the O_3 partial pressures are smaller and the profiles peak at a lower pressure.

The final series of tests was a simultaneous error study to obtain a more realistic estimate of the O_3 partial pressure accuracy which might be expected from the horizon experiment. The conditions of Table 2 were imposed simultaneously using the Thule, Greenland, radiances. The error limits given in this table are either presently attainable or the values will most likely be possible in the future. Excluding random errors, the B set of values are all additive in effect. Thus, these correspond to an unfavorable case. The A set of errors is identical to the B set with the exception of tangent height error which is opposite in sign. Thus, in the A set, the effect of tangent height error tends to cancel effects caused by other errors and this corresponds to a favorable case. The radiance errors are conservative values since each is greater than the value estimated to be currently possible by McKee *et al.* (1969b). The tangent height and surface pressure errors are realistic values at the present time, and the O_3 absorption line intensity error should be achievable in the future. The temperature bias error was set equal to zero for these calculations and a random temperature error was used in its place. Although temperature bias errors probably will never be exactly zero, they should be minimized in a properly designed experiment. The results of inversions using errors in Table 2 are shown in Figs. 11 and 12, respectively. The circles are the O_3 partial pressures determined in the inversion for each tangent point. The radiance values were smoothed in these calculations using the segmented quadratic least-squares technique previously described. The case B inversion is unstable for pressures $\gtrsim 150$ mb. In the range 1–25 mb (50–25 km) most case B inversion points are within 20% or less of the actual sounding. A few points are in error by 28% or greater and two are in error by more than 40%. For the same pressure range

in case A, most points are within 15% or less of the true profile, some are in error by about 20% and two points are in error by 30% or greater. When Green's ozone profile function (Green, 1964) was least-squares fitted to each solution (cases A and B) in the range 1–25 mb, all points on the curve were within 10% or less of the true profile in both cases. These errors give a root mean square (rms) range from 15–20% for the unsmoothed solutions and an rms value of 5% for the smoothed results. However, it should be emphasized that these calculations were done using a zero temperature bias error. Since a temperature bias of only 3K would critically degrade these results, great stress should be placed on methods of minimizing this source of error in an experiment.

The ozone horizon experiment is compared with three other techniques in Table 3. As shown, the infrared horizon approach is the only method which is applicable on both the day and night side of the planet and it is the only technique which provides middle and upper stratospheric ozone data during the night. Furthermore, it extends the lower altitude limit for determining O_3 partial pressure from a satellite and thereby complements the other methods.

There have been several recent developments in critical areas of the horizon experiment. McKee (1970) has suggested a method of eliminating the need for accurate pointing through simultaneous inference of temperature and pressure. A similar, but improved, approach has also been developed by investigators in the Nimbus F limb-radiance inversion experiment and it now appears that the general temperature-pressure inference technique is feasible (Gille and House, 1971). Preliminary results indicate that equivalent pointing accuracy will be much better than the ± 1 km used in this study. Also, it now seems feasible, because of new advances in instrumentation technology, to achieve significant improvements in radiance accuracies over those used in this analysis. It may be possible, for example, to reduce the random radiance noise by a factor of 5 (Gille and House, 1971). If such improvements can be obtained, the final errors in inferred O_3 concentrations will be smaller than those indicated by the simultaneous error study. It should also be possible to extend the altitude range of the horizon experiment to include the range from approximately 60 km down to the tropopause region.

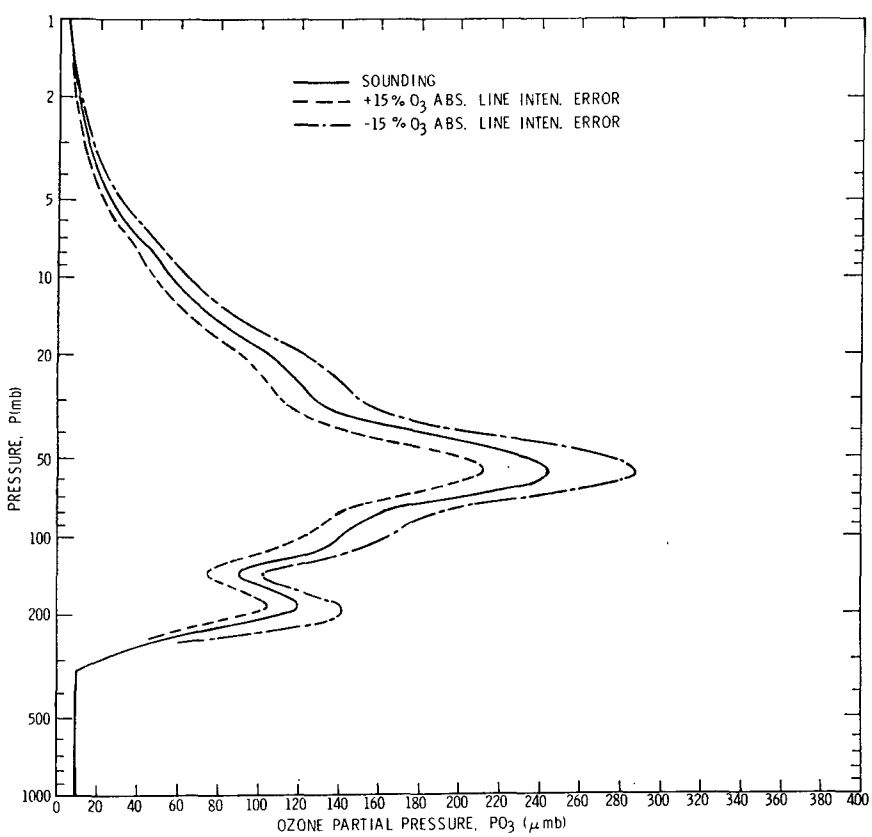

FIG. 9. Ozone absorption line intensity error results for Thule, Greenland (76.5N), 19 May 1965.

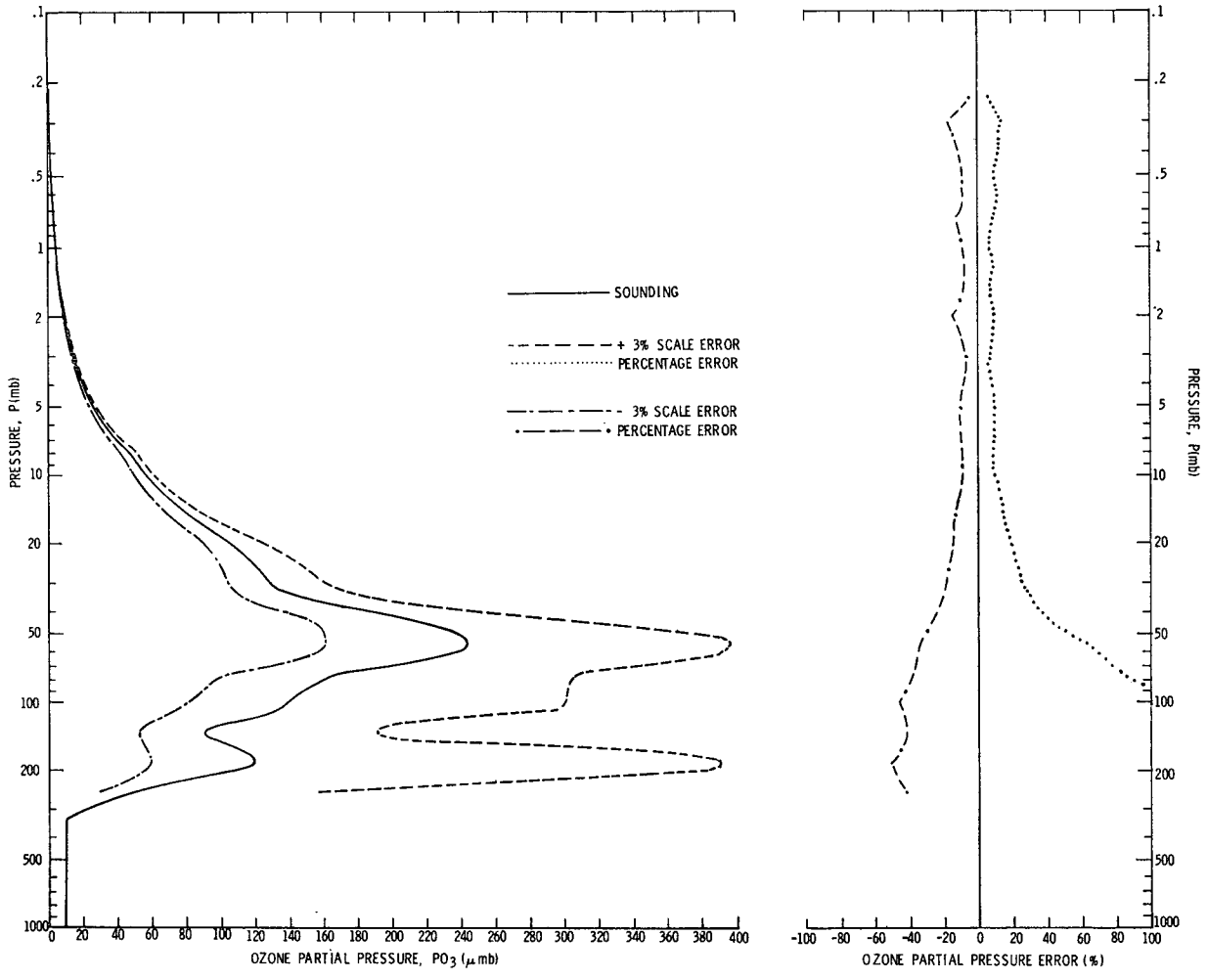

FIG. 10. Radiance scale error results for Thule, Greenland (76.5N), 19 May 1965.

4. Conclusions

A method has been presented for inferring ozone information from satellite horizon measurements in the 1042 cm^{-1} band. An analysis of the horizon experiment using this method revealed that the O_3 partial pressure can be determined in the altitude range from 50 km down to approximately 25 km. The top limit arises because of the small optical depth of the atmosphere in the upper layers and the bottom extreme occurs because the atmosphere is almost opaque in the lower layers. A study of individual error effects using a high-latitude synthetic radiance profile showed that inversions will be poor unless the atmospheric temperature profile can be accurately determined. The O_3 partial pressure errors for temperature bias errors of only ± 3K were approximately $\pm 30\%$ in the upper stratosphere and deteriorated to -40% and $+100\%$ at 25 km. The next most significant error effect in an experiment would be caused

TABLE 2. Types and ranges of errors used in the horizon experiment simultaneous error study.

Type of error	Range A*	Range B*
Random radiance noise normally distributed with a mean of zero	$\sigma = 0.02$ W $(m^2\text{-sr})^{-1}$	$\sigma = 0.02$ W $(m^2\text{-sr})^{-1}$
Radiance bias	0.02 W $(m^2\text{-sr})^{-1}$	0.02 W $(m^2\text{-sr})^{-1}$
Radiance scale	2%	2%
Tangent height	-1 km	1 km
Ozone absorption line intensity	-4%	-4%
Surface pressure	-2%	-2%
Temperature bias	none	none
Random temperature normally distributed with a mean of zero	$\sigma = 3$K	$\sigma = 3$K

* Set A, a favorable arrangement of errors; set B, an unfavorable arrangement. See text for discussion.

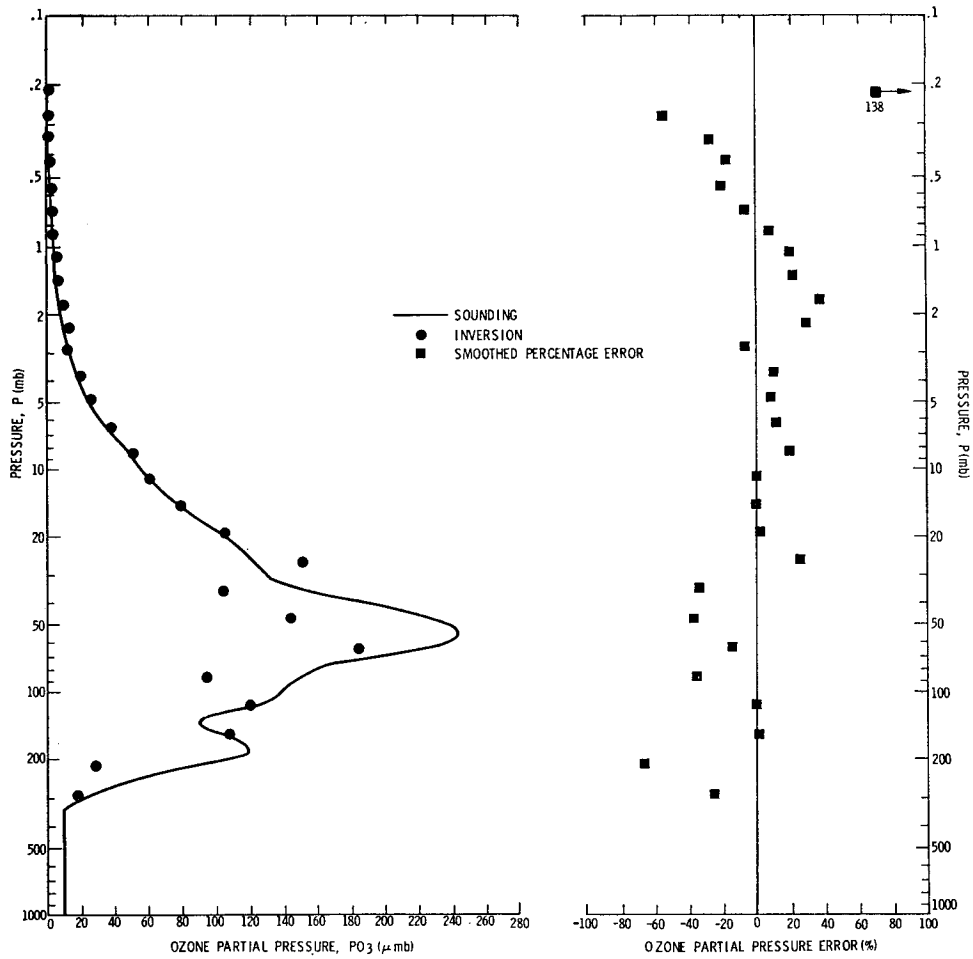

FIG. 11. Case A simultaneous error study results for Thule, Greenland (76.5N), 19 May 1965. See text for discussion.

TABLE 3. A comparison of different satellite methods for measuring high-altitude atmospheric ozone.

Method	Range (km)	Comments	References
Measurement of infrared radiation coming from the horizon	25 to 50	Applicable on both the day and night side of the planet.	This report
Measurement of backscattered UV solar radiation*	35 to 55	Applicable only on the day side of the planet.	Singer and Wentworth (1957); Sekera and Dave (1961); Twomey (1961); Dave and Mateer (1967); Herman and Yarger (1969); Anderson *et al.* (1969);
Measurement of visible and near UV solar radiation passing tangentially through the atmosphere**	45 to 65	Applicable only on the day side of the planet.	Frith (1961); Rawcliffe *et al.* (1963); Duardo (1967); Miller (1969)
Measurement of a stellar UV spectrum during occultation from a satellite	40 to 100	Applicable only on the night side of the planet.	Hays and Roble (1967)

* This method may be extended to a lower altitude in the future if current difficulties caused by multiple scattering can be reduced or eliminated.

** Since there are only two measurement points per orbit, many satellites would be required to obtain wide geographic coverage.

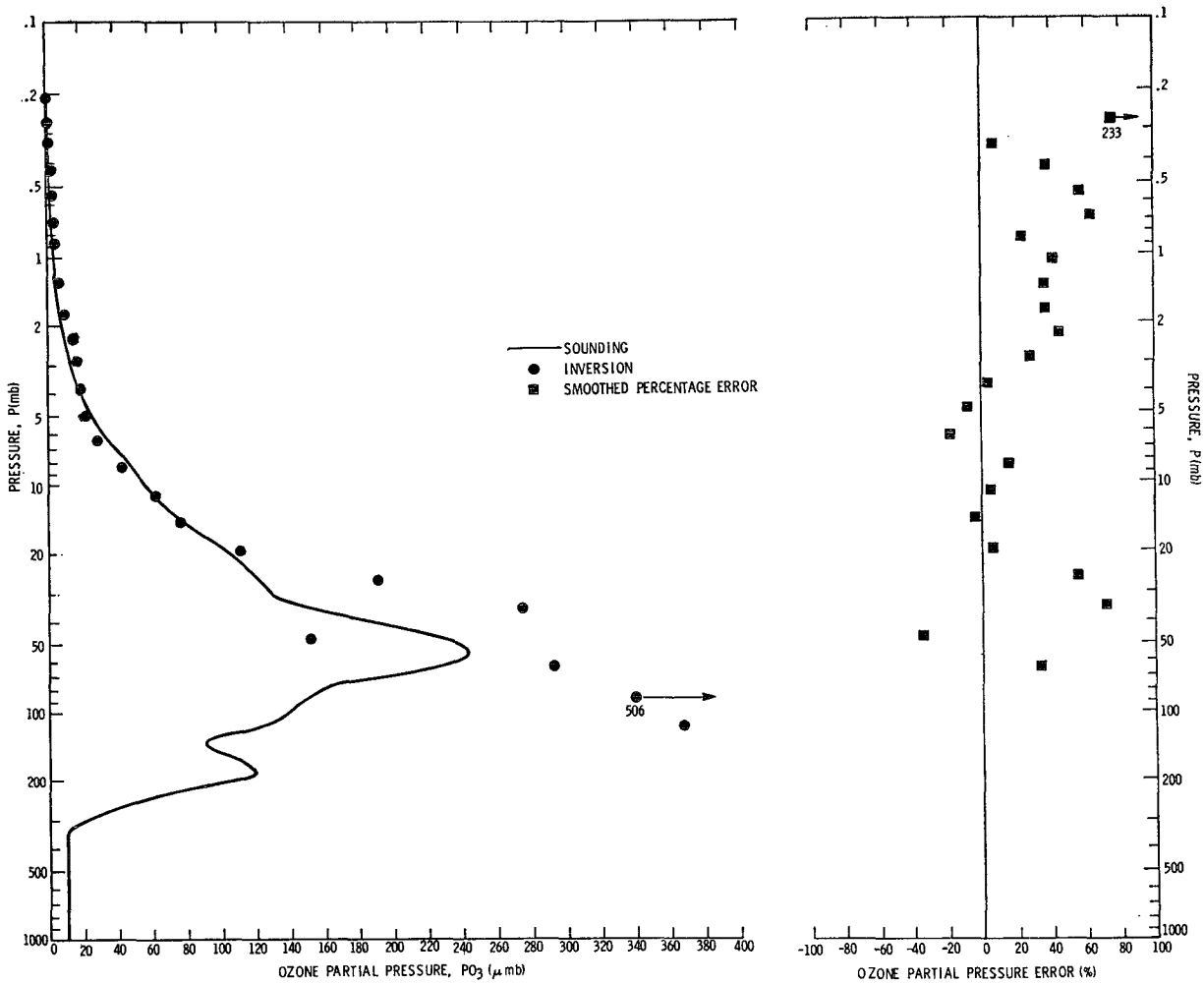

FIG. 12. Same as Fig. 11 except for Case B.

by tangent height errors. The error study showed that ± 1 km errors caused O_3 partial pressure errors of about 16% throughout most of the applicable altitude range. The maximum effect due to any other error source probably will not exceed 7% at 25 km in an actual experiment. All ozone errors were slightly less for a similar study performed with a low-latitude synthetic radiance profile. The last set of calculations was a simultaneous error study. The temperature bias error was set equal to zero for these calculations and normally distributed random temperature errors were used instead with a standard deviation of 3K. The results showed that it should be possible to determine the O_3 partial pressure to within rms limits of 15–20% in the range 25–50 km. It may be possible to reduce this error to 5% by smoothing the solution profile. Since a temperature bias error of only 3K would critically degrade these results, great stress should be placed on methods of minimizing this source of error in an experiment. It seems likely, in view of recent technological developments, that final ozone errors will be smaller than the above values and the altitude range will be greater, i.e., from ~60 km down to the tropopause region.

Acknowledgments. This research was originally presented as part of a University of Michigan Ph.D. dissertation submitted by the first author in July 1970. The work was supported by the National Aeronautics and Space Administration under Contract NGR 23-005-394 and by the National Oceanographic and Atmospheric Administration under Contract E92-69-N.

REFERENCES

Anderson, G. P., C. A. Barth, F. Cazla and J. London, 1969: Satellite observations of the vertical ozone distribution in the upper stratosphere. *Ann. Geophys.*, **25**, No. 1, 341–345.

Armstrong, B. H., 1968: Analysis of the Curtis-Godson approximation and radiation transmission through inhomogeneous atmospheres. *J. Atmos. Sci.*, **25**, 312–322.

Bates, J. C., D. S. Hanson, F. B. House, R. Carpenter and J. Gille, 1967: The synthesis of 15 μ infrared horizon radiance profiles from meteorological data inputs. Contractor Rept. NASA CR-724.

Burn, J. W., and W. G. Uplinger, 1969: The determination of atmospheric temperature profiles from planetary limb radiance profiles Rept. LMSC-681950, NASA Contract NAS1-8048, Lockheed Missiles and Space Co.

Chandrasekhar, S., 1960: *Radiative Transfer*. Dover Publ., New York.

Clough, S. A., and F. X. Kneizys, 1965: Ozone absorption in the 9.0 micron region. Physical Sciences Research Paper No. 170, Air Force Cambridge Research Laboratories.

Dave, J. V., and C. L. Mateer, 1967: A preliminary study on the possibility of estimating total atmospheric ozone from satellite measurements. *J. Atmos. Sci.*, **24**, 414–427.

Davis, R. E., 1969: A limb radiance calculation approach for model atmospheres containing horizontal gradients of temperature and pressure. Tech. Note NASA TN D-5495.

Dobson, G. M. B., 1930: Observations of the amount of ozone in the earth's atmosphere and its relations to other geophysical conditions. Part IV. *Proc. Roy. Soc., London*, **A129**, 411–433.

Drayson, S. R., 1966: Atmospheric transmission in the CO_2 band between 12 μ and 18 μ. *Appl. Opt.*, **5**, 385–391.

Duardo, J. A., 1967: Study to develop a technique for measurement of high altitude ozone parameters. Tech. Rept. N67-28366, Contract NAS 12-137, Electro-Optical Systems, Inc.

Fabry, C., and M. Buisson, 1913: L'absorption de l'ultraviolet par l'ozone et la limit du spectra solaire. *J. Phys. Radium*, **3**, 196.

Frith, R., 1961: Measuring the ozone above the earth. *Discovery*, 390–391.

Gille, J. C., 1968: On the possibility of estimating diurnal temperature variation at the stratopause from horizon radiance measurements. *J. Geophys. Res.*, **73**, 1863–1868.

——, and R. G. Ellingson, 1968: Correction of random exponential band transmissions for Doppler effects. *J. Appl. Opt.*, **7**, 471–474.

——, and F. B. House, 1971: The inversion of limb radiance measurements I. Temperature. *J. Atmos. Sci.*, **28**, 1427–1442.

Godson, W. L., 1960: Total ozone in the middle stratosphere over arctic and sub-arctic areas in winter and spring. *Quart. J. Roy. Meteor. Soc.*, **86**, 301–317.

Goody, R. M., 1952: A statistical model for water-vapor absorption. *Quart. J. Roy. Meteor. Soc.*, **78**, 165–169.

——, 1964: *Atmospheric Radiation I: Theoretical Basis*. Oxford University Press, 436 pp.

Green, A. E. S., 1964: Attenuation by ozone and the earth's albedo in the middle ultraviolet. *Appl. Opt.*, **3**, No. 2, 203–208.

Hays, P. B., and R. G. Roble, 1967: Stellar spectra and atmospheric composition. Rept. No. 08953-1-T, College of Engineering, University of Michigan.

Hering, W. S., and T. R. Borden, 1967: Ozonesonde observations over North America, Vol. 4. Environmental Res. Paper No. 279, AFCRL-64-30(IV).

Herman, B. M., and D. N. Yarger, 1969: Estimating the vertical atmospheric ozone distribution by inverting the radiative transfer equation for pure molecular scattering. *J. Atmos. Sci.*, **26**, 153–162.

House, F. B., and G. Ohring, 1969: Inference of stratospheric temperature and moisture profiles from observations of the infrared horizon. Contractor Rept. NASA CR-1419.

Kuhn, W. R., and J. London, 1969: Infrared radiative cooling in the middle atmosphere (30–110 km). *J. Atmos. Sci.*, **26**, 189–204.

McKee, T. B., 1970: Inference of temperature and water vapor structure in the stratosphere from limb radiance profiles. NASA TM X-1943.

——, R. I. Whitman and J. J. Lambiotte, 1969a: A technique to infer atmospheric temperature from horizon radiance profiles. NASA TN D-5068.

——, —— and ——, 1969b: A technique to infer atmospheric water-vapor mixing ratio from measured horizon radiance profiles. NASA TN D-5252.

Miller, D. E., 1969: The measurement of ozone from a satellite. Paper presented at the NATO/British Interplanetary Society, International Summer School on Earth Observation Satellites, Cambridge, England, 14–25 July.

National Academy of Sciences, 1965: Atmospheric ozone studies—An outline for an international observation program. Publ. No. 1348.

Paetzold, H. K., 1953: The mean vertical ozone distribution resulting from the photochemical equilibrium, turbulence, and currents of air. *J. Atmos. Terr. Phys.*, **3**, 125–131.

Prabhakara, C., 1969: Feasibility of determining atmospheric ozone from out-going infrared energy. *Mon. Wea. Rev.*, **97**, 307–314.

——, B. J. Conrath, R. A. Hanel and E. J. Williamson, 1970: Remote sensing of atmospheric ozone using the 9.6 μ band. *J. Atmos. Sci.*, **27**, 689–697.

Rawcliffe, R. D., G. E. Meloz, R. M. Friedman and E. H. Rogers, 1963: Measurement of the vertical distribution of ozone from a polar orbiting satellite. *J. Geophys. Res.*, **68**, 6425–6429.

Russell, J. M., 1970: The measurement of atmospheric ozone using satellite infrared observations in the 9.6 μm band. Rept. No. 03635-1-T, College of Engineering, University of Michigan.

Sekera, Z., and J. V. Dave, 1961: Determination of the vertical distribution of ozone from the measurement of diffusely reflected ultraviolet solar radiation. *Planetary Space Sci.*, **5**, 122–136.

Sekihara, K., and C. D. Walshaw, 1969: The possibility of ozone measurements from satellites using the 1043 cm^{-1} band. *Ann. Geophys.*, **25**, No. 1, 233–241.

Singer, S. F., and R. C. Wentworth, 1957: A method for the determination of the vertical ozone distribution from a satellite. *J. Geophys. Res.*, **62**, 299.

Smith, O. E., W. M. McMurray and H. L. Crutcher, 1963: Cross sections of temperature, pressure, and density near the 80th meridian west. NASA TN D-1641.

Twomey, S., 1961: On the deduction of the vertical distribution of ozone by ultraviolet spectral measurements from a satellite. *J. Geophys. Res.*, **66**, 2153–2162.